Korean J. of Chem. Eng., **11**(2), 81-88 (1994)

A STUDY ON FLOW CHARACTERISTICS IN A ROTATING SCREEN BLADE EXTRACTION COLUMN

Young Kook Choi* and Chul Kim

Dept. of Chem. Eng., Ajou University, Suwon 441-749, Korea

(Received 2 March 1993 • accepted 2 December 1993)

Abstract—Studies have been carried out on the axial dispersion in the continuous phase and the hold-up of dispersed phase in a rotating screen-blade extraction column, by employing an axial dispersion model. Experiments on both single and two phase operations have been conducted with the plate spacing, the mesh size, the impeller speed (RPM), and the superficial velocities as the system parameters. By regression analysis of experimental data, empirical equations correlating the dispersion coefficients and the fractional hold-up of dispersed phase with the system parameters were obtained.

INTRODUCTION

In the design of continuous countercurrent liquid-liquid extraction columns, the general objectives are to achieve a high mass transfer effectiveness and a high throughput in relation to the column size. To achieve these, the externally agitating components are adopted, which supply additional energy for creating a large specific interfacial area and generating turbulence. External agitation can be applied in many ways; by rotary stirrers [1-4], rotating discs [5, 6], reciprocating plates [7-9], pulsation [10, 11] and others, which greatly enhance the interfacial contact area by breaking up the dispersed droplets. As the agitation intensity is increased, however, axial mixing tends to reduce the effectiveness of any countercurrent mass transfer process by flattening the axial concentration gradients in each phase and thus reducing the overall driving force. This effect leads to a growing volume of countercurrent columns allowing the backmixing.

Also, in the scale up of an extraction column the axial dispersion effect may increase with column diameter resulting in a less effective performance on the large scale than predicted on the basis of constant throughput and energy input [12]. In some extraction columns, it has been indicated that the scale up of the columns should be possible without increasing the height of the columns [13, 14].

An important factor in understanding the fundamental mass transfer mechanisms in an extraction column is the effect of axial dispersion or residence time distribution (RTD) of the continuous phase. The best reasonable values of Peclet number and holding time are obtained experimentally by injecting an impulse of tracer and measuring the change in concentration profile as it passes through the column. The axial dispersion coefficients in the continuous phase are determined from these values.

Much work is concerned with the axial mixing effect in an agitated impeller column. However, studies on the overall mass transfer, the hold-up and the flow characteristics of a rotating screen-blade extraction column have not been given much consideration. A less power requirement and more beneficial effect of increased interfacial area as compared to an agitated impeller column may be achieved in the rotating screen-blade extraction column.

The primary objective of this study is to determine experimentally, the axial dispersion coefficients in the continuous phase by an impulse tracer technique and to obtain empirical equations correlating the system parameters by regression analysis of experimental data.

THEORETICAL

1. Axial Dispersion Model

Dispersion models have been widely used to depict the flow and mixing characteristics of a flow system [15, 16]. These models have been used mainly to describe the flow in empty tubes and packed beds; sys-

*Korea Research Institute of Chemical Technology, Taejon, Korea

tems in which the velocity profiles are closer to plug flow. Under the assumptions of negligible radial gradient and a constant axial dispersion coefficient, a dispersion model can be described by the equation,

$$\frac{\partial C_i}{\partial t} + u\frac{\partial C_i}{\partial x} = E_c\frac{\partial^2 C_i}{\partial^2 x} + S_i + r_i \tag{1}$$

where

C_i = the time-averaged concentration of species i,
E_c = the axial dispersion coefficient,
S_i = the rate of input of species i from sources,
u = the axial velocity, and
r_i = the rate of generation of species i by chemical reaction.

In tracer experiments without chemical reaction, $r_i = 0$, and the source term is given by

$$S_i = \frac{I}{\Pi}\delta(x - x_o)\ f(R)$$

where

I = injection rate of tracer, $\delta(X - X_o)$ = Dirac-delta function,

$$f(R) = \begin{cases} 1/R_i^2, & R \le R_i \\ 0, & R_i \le R, \text{ and} \end{cases}$$

R_i = injector tube radius.

In dimensionless variables, Eq. (1) has the form;

$$\frac{\partial C}{\partial \Theta} + \frac{\partial C}{\partial Z} = \frac{1}{P}\frac{\partial^2 C}{\partial Z^2} + \delta[(Z - Z_o)]\delta(\theta) \tag{2}$$

where

$\Theta = ut/L = Ft/V$, $Z = x/L$, $P = uL/Ec$ (Peclet number), and $C = C/C_o$.

From Eq. (2) Van der Lann [17] obtained the moments at $Z = Z_m (Z_o < Z_m < Z_e)$ for general boundary conditions;

$$\mu_1 = 1 + \frac{1}{P}[2 - (1-a)\exp(-PZ_o)] - (1-b)\exp[-P(Z_t - Z_m)] \tag{3}$$

$$\sigma^2 = \frac{2}{P} + \frac{1}{P^2}[8 + 2(1-a)(1-b)\exp(-Z_e) - (1-a)\exp(-PZ_o)\{4Z_oP + 4(1+a) + (1-a)\exp(-PZ_o)\} - (1-b)\exp\{-P(Z_e - Z_m)\}[4(Z_e - Z_m)P + 4(a+b)] + (1-b)\exp\{-P(Z_e - Z_m)\}] \tag{4}$$

where $a = P/P_a$ and $b = P/P_b$,
Z_o = injection point, and
Z_e = end of column test section.

Aris [18], Bischoff [19], Jeong [20], Kim [21] and Bischoff and Levenspiel [22] utilized the output tracer concentrations for an imperfect delta input signal measured at two points Z_o and Z_m both within the test section, and calculated the moments;

$$\Delta\mu_1 = 1 - \frac{1-b}{P}\{1 - \exp(-P)\}\exp\{P(Z_m - Z_e)\} \tag{5}$$

$$\Delta\sigma^2 = \frac{2}{P} + \frac{1-b}{P^2}\exp\{P(Z_m - Z_e\}\{4(1+b) \{\exp(-P) - 1\} + [4P(Z_m - Z_e) + (1-b)\{\exp(-2P) - 1\}\exp\{P(Z_m - Z_o)\} + 4P(Z_m - Z_o)\exp(-P)] \tag{6}$$

2. Analysis of the Response Curve

Because of the long tail, the response curves have been divided into two sections in obtaining the deterministic moments. The tail section could be described by an exponential decay function [20]

$$C = C_A\ \exp\{-K(t - t_A)\}$$

where C_A is the dimensionless concentration obtained when C reaches one-sixth (1/6) of C_{max} at $t = t_A$, and K is a decay factor. The parameter K is evaluated from the tail section of the response curve and found approximately in the range of $C_{max}/30$ and $C_{max}/6$. This procedure leads to the following deterministic moments;

$$\alpha = \sum_{i=0}^{n} C_i\Delta t + \frac{C_T}{K} \tag{7}$$

$$\mu = \frac{1}{\alpha}\left[\sum_{i=0}^{n} C_i t_i \Delta t + \frac{C_T}{K}\left(t_c + \frac{1}{K}\right)\right] \tag{8}$$

$$\sigma^2 = \frac{1}{\alpha}\left[\sum_{i=0}^{n} C_i t_i \Delta t + \frac{C_T}{K}\left(t_c^2 + \frac{2t_c}{K} + \frac{2}{K^2}\right)\right] - \mu_1^2 \tag{9}$$

where $C_T = C_{max}/30$ at $t = t_c$.

3. Regression Analysis and Response Surface Methodology

In multiple linear regression, the regression equation can be written as

$$y_i = \beta_o + \beta_1 X_{1j} + \beta_2\ X_{2j} + \cdots + \beta_k\ X_{kj} + \varepsilon_j = \beta_o + \sum_{i=1}^{k} \beta_i\ X_{ij} + \varepsilon_j \qquad j = 1, 2, \cdots, n \tag{10}$$

The estimation procedure requires that the random error components have $E(\varepsilon) = 0$, and $Var(E) = \sigma^2$.

The response surface methodology is a combination of mathematical and statistical techniques useful for analyzing problems where several independent variables influence the dependent variables or the response, and the goal is to optimize this response.

The independent variables in this study are the Peclet number P and the holding time $\bar{t}$. They were obtained by the parameter estimation using deterministic moments and are taken as the first values, and in the two level factorial design the two levels of interest are set to be -5% and $+5\%$ [20-23].

Using the independent variables coded to a $(-1, 1)$ interval and the two-level factorial design, the steepest path is obtained. In terms of four data, the regression Eq. (10) can be written as

$$y_i=\beta_o+\beta_1 X_{ij}(P)+\beta_2 X_{ij}(\bar{t})+\varepsilon_i \quad (j=1, 2, 3, 4) \tag{11}$$

Putting in matrix notation, Eq. (11) can be written as

$$Y=X/\beta+E$$

where

$$Y=\begin{bmatrix} y_1 \\ y_2 \\ y_3 \\ y_4 \end{bmatrix} \qquad X=\begin{bmatrix} 1 & +1 & +1 \\ 1 & -1 & +1 \\ 1 & +1 & -1 \\ 1 & -1 & -1 \end{bmatrix}$$

$$/\beta=\begin{bmatrix} \beta_o \\ \beta_1 \\ \beta_2 \end{bmatrix} \quad \text{and} \quad E=\begin{bmatrix} \varepsilon_1 \\ \varepsilon_2 \\ \varepsilon_3 \end{bmatrix}$$

The components of the least square estimator are found;

$$\beta_o=(y_1+y_2+y_3+y_4)/4$$
$$\beta_1=(y_1-y_2+y_3-y_4)/4$$
$$\beta_2=(y_1+y_2-y_3-y_4)/4 \tag{12}$$

EXPERIMENTAL

The overall schematic flow diagram is shown in Fig. 1. The heavy and light phases were fed to the column close to the first stator ring (doughnut type plate) from the head tank equipped with an overflow outlet to maintain the liquid level constant. The continuous phase outlet is equipped with an adjustable limb to maintain constant interface level, and the dispersed phase outlet is equipped with an overflow. The rotaing unit is connected to the top of the main column. Solenoid valves are installed at the inlet and outlet of the column in order to stop the flows simultaneously.

The main extraction column is made of pyrex glass of 6.55 cm inside diameter with an overall height of 220 cm. The top and bottom sections of the main column are made of 13.5 cm inside diameter lucite column segments of 23 cm and 27 cm length, respectively. The main column is provided with the injection

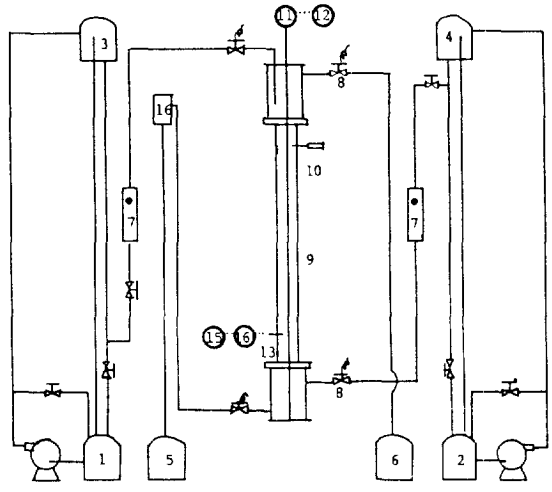

Fig. 1. Schematic flow diagram.

1. Aqueous storage tank	2. Organic storage tank
3. Aqueous head tank	4. Organic head tank
5. Aqueous reservoir	6. Organic reservoir
7. Rotameter	8. Solenoid valve
9. Main column	10. Sampling needle
11. D.C. motor	12. Speed adjuster
13. Conductivity cell	14. Wheatstone bridge
15. Recorder	16. Level adjuster

Table 1. Description of system

Column	Effective height (cm)	200
	Inside diameter (cm)	6.5
	Opening diameter of stator (cm)	4.5
	Impeller diameter (cm)/ width (cm)	4.4/1.5
	Impeller type	Screen-blade
System	Continuous phase	Distilled water
	Dispersed phase	Refined kerosene
	Tracer	KCl

ports at 20 cm intervals on one side and at two, 200 cm apart on the other side.

The doughnut plates and the screen blade impeller are made of 1 mm thick SUS304 stainless steel plates (Table 1). The doughnut type plates are supported in the main column by means of three 220 cm length rods of 3.5 mm diameter. Stainless steel sleeves around the rod serve as spacers for the plates. The spacer plays a role to adjust the compartment height. The impeller are fixed by a 10 mm diameter 296 cm length stainless steel rod. Four little bearings are installed to keep the rod free from vibration. The entire rod assembly can be set by lifting it from the open top

Table 2. Experimental variables

Variable	Range
Mesh size (NO)	10-50
Impeller speed (N, RPM)	120-480
Compartment height (H, cm)	5-9
Velocity of water (U_c, cm/min)	7.42-22.26
Velocity of kerosene (U_d, cm/min)	7.42-22.26

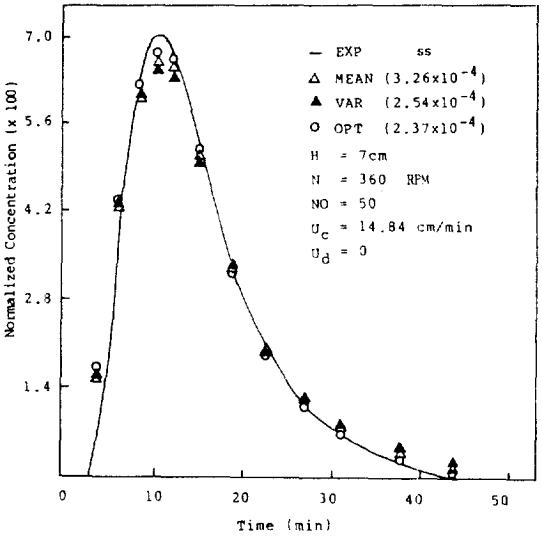

Fig. 2. Residence time distribution (RTD)-experimental vs. theoretical-.

of the column. The shaft rod is driven by the pulley attached to an impeller speed adjuster driven by a 1/4 hp 110 volt D.C. motor.

The column was initially filled with the heavy phase (distilled water) set at the desired flow rate, and the rotating unit was set in operation maintaining a proper impeller speed. The light phase (refined kerosene) set at the desired flow rate was then gradually introduced.

When steady state was reached, an half second impulse of 0.5 N potassium chloride was carefully injected into the main column using a syringe at an injection port. Concentrations of the tracer were measured at sampling port by a conductivity bridge network. The conductivity probe is made of 5 mm width and 5 mm length platinum plate.

Hold-up measurements were made when two phases were completely separated after the solenoid valves were shut off in order to stop the flows. Experimental conditions are listed in Table 2.

RESULT AND DISCUSSION

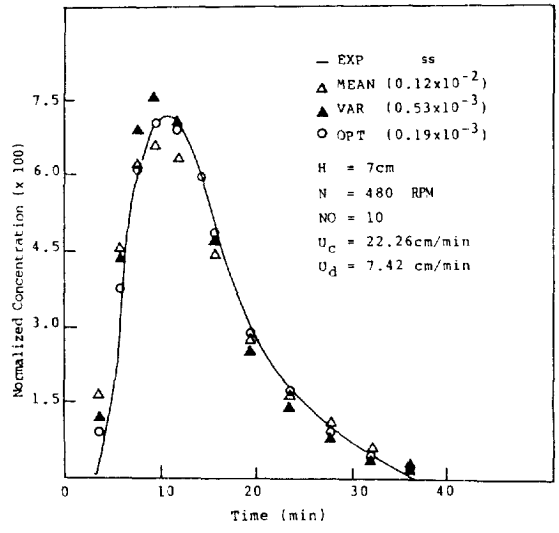

Fig. 3. Residence time distribution (RTD)-experimental vs. theoretical-.

While a dispersion model has been commonly employed for flows in pipes, packed beds and others where discrete stages were not readily identified, the application of this model has been attempted to the present system considering the interchange of liquid between the free area of interplate regions.

The typical results of the moment analysis are compared with the experimental data for single and two phase operations in Figs. 2 and 3 where the mean (MEAN), the variance (VAR) and the optimized (OPT) values are shown. Also specified in the Figs. are the system parameters and experimental conditions including the velocities of both continuous and dispersed phases, U_c and U_d. The value of the sample variance (ss) in the regression analysis was lower than those for moment analyses, hence, in good agreement with response curves.

1. Single Phase Correlation

The effects of the mesh size or the mesh number NO and the impeller speed N on the axial dispersion coefficient Ec are shown in Fig. 4. The dispersion coefficient tends to increase with increasing these parameters which are the determining factors for mixing. When mechanical agitation is applied to enhance mixing, a part of fluid recirculates and is mixed to the fluid in adjacent stage opposite to main flow, resulting in the backmixing that is expected to increase with mixing intensity.

The degree of backmixing could be estimated by an axial dispersion coefficient which is significantly affected by the mesh size and the impeller speed. This

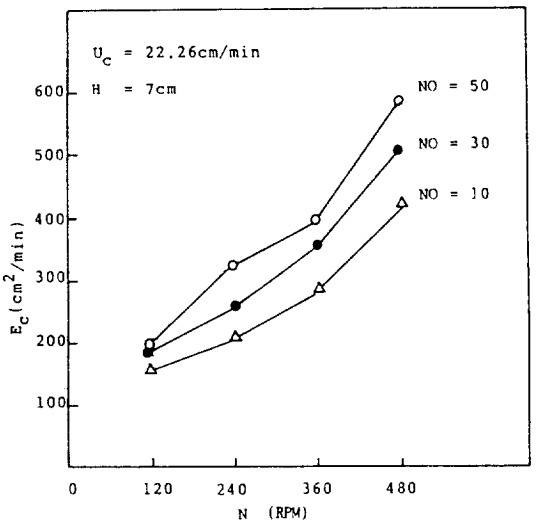

Fig. 4. Effect of RPM on axial disperison coefficient (single phase).

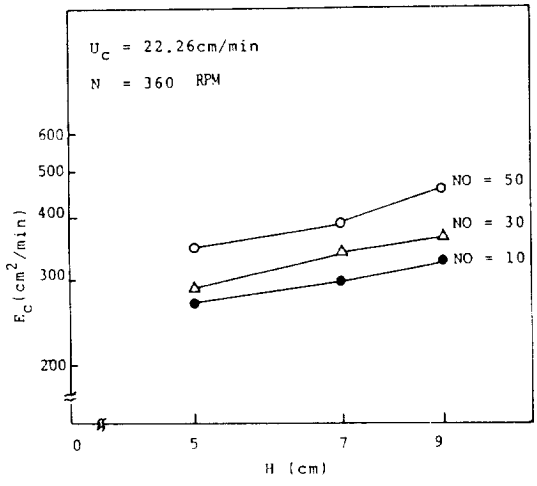

Fig. 5. Effect of compartment height on axial dispersion coefficient (single phase).

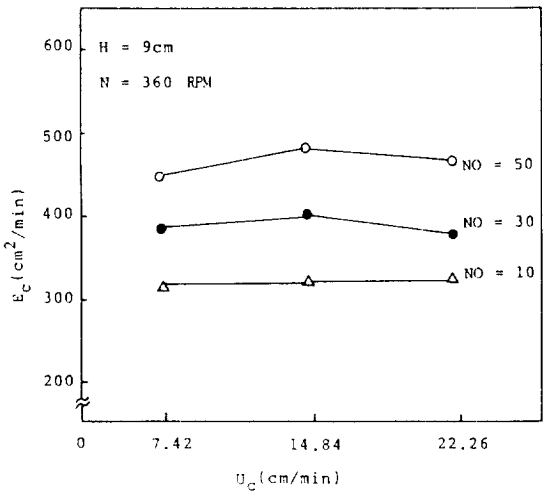

Fig. 6. Effect of continuous phase superficial velocity on axial dispersion coefficient (single phase).

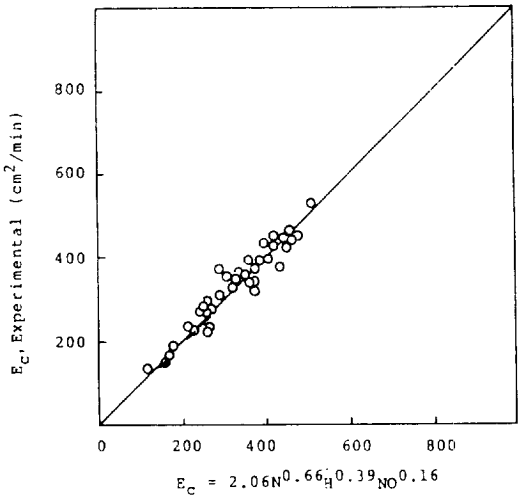

Fig. 7. Correlation of axial dispersion coefficient (single phase).

trend is in accordance with the most previous data for agitated impeller columns of different types [20] and rotary disc columns [6].

The compartment height H was found to have a positive effect on the axial dispersion coefficient as illustrated in Fig. 5. The axial dispersion coefficient increased with the plate spacing and this trend is in accordance with previous data for agitated impeller columns [3, 20].

In the column used in this study in turbulence level tends to incline with an increase in plate spacing leading to the present results.

The effect of the continuous phase superficial velocity is shown in Fig. 6. The continuous phase superficial velocity has no significant effect on the axial dispersion coefficients. This trend corresponds to the previous data for the reciprocating column [7] and agitated impeller column [21]. On the other hand, a minor effect was observed in the study of Bibaud [3] and in the data for the rotary disc column [24].

The axial dispersion coefficient was correlated with the mesh size, the impeller speed, the continuous phase superficial velocity and the plate spacing. Noting that the effect of the continuous phase superficial ve-

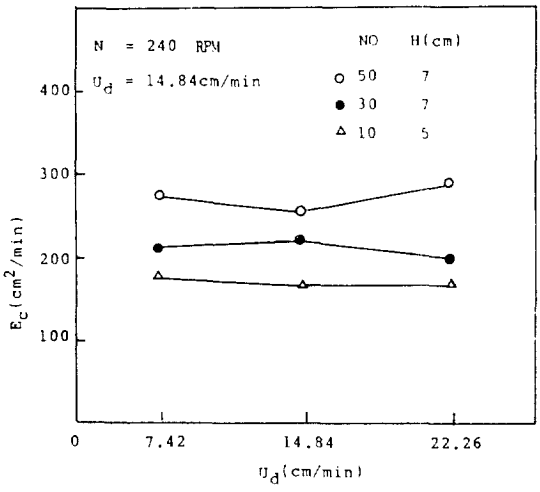

Fig. 8. Effect of dispersed phase superficial velocity on axial dispersion coefficient (two phase).

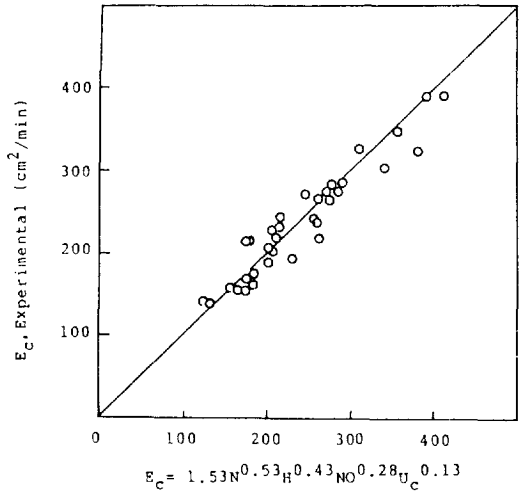

Fig. 9. Correlation of axial dispersion coefficient (two phase).

locity is insignificant, the following expression was obtained by the regression analysis of experimental data.

$$E_c = 2.06\ N^{0.66}\ H^{0.39}\ NO^{0.16}. \quad (13)$$

The results are shown in Fig. 7.

2. Two Phase Correlation

Experimental data was obtained in the emulsion flow regime in which the dispersed phase droplets moved freely within the continuous phase. There was only a minor indication of clustering and coalescence near the doughnut plates during agitation.

The effects of the mesh size, the impeller speed, the plate spacing, and the continuous phase superficial velocity, U_c on the axial dispersion coefficients, have been correlated. Noting also that the effect of the superficial velocity of the dispersed phase was negligible on the axial dispersion coefficients as shown in Fig. 8, the regression analysis was carried out excluding the dispersed phase superficial velocity to obtain;

$$E_c = 1.53\ N^{0.53}\ H^{0.43}\ NO^{0.28}\ U_c^{0.13} \quad (14)$$

The results are shown in Fig. 9.

3. Hold-up

The size of kerosene droplets decreased with increasing the mesh size and the impeller speed in two phase operation. Thus the difference in density of two phases decreased and the volume fractional hold-up of the dispersed phase Φ_d in each stage increased.

Observing the insignificant effect of the continuous phase superficial velocity on the fractional hold-up, the experimental data were correlated resulting in an expression;

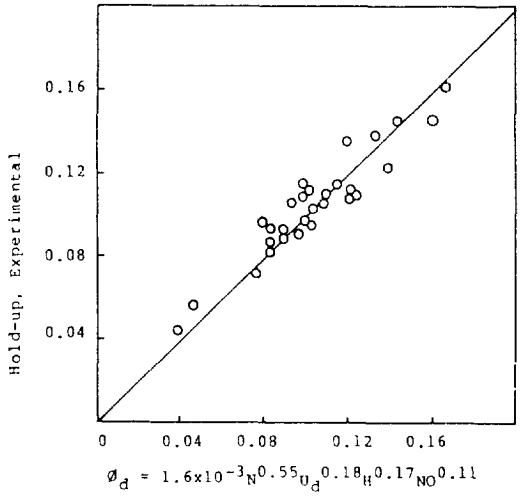

Fig. 10. Correlation of dispersed phase hold-up ratio (organic/total).

$$\Phi_d = 1.6\times10^{-3}\ N^{0.55}\ U_d^{0.18}\ H^{0.17}\ NO^{0.11} \quad (15)$$

The results are shown in Fig. 10.

From this equation it is apparent that the dispersed phase hold-up is strongly influenced by the impeller speed.

CONCLUSIONS

An axial dispersion model has been found satisfactorily applicable in depicting the flow characteristics in a rotating screen-blade extraction column. The axial

dispersion coefficients in the continuous phase and the dispersed phase hold-up have been successfully correlated with the system parameters, the impeller speed, the plate spacing or the compartment height, the mesh size and the velocities of the continuous and the dispersed phases. The empirical equations obtained by regression analyses show that the effect of the continuous phase superficial velocity is negligible in single phase operation whereas the effect is rather significant in two phase operations. Also noted is the effect of the dispersed phase superficial velocity on the fractional hold-up of the dispersed phase.

NOMENCLATURE

a : P/P_a [-]
b : P/P_b [-]
c : tracer concentration [g-mole/cm^3]
C : dimensionless tracer concentration (c/c_o) [-]
C_A : dimensionless tracer concentration when $C=(1/6)C_{max}$, at $t=t_A$ [-]
C_T : dimensionless tracer concentration when $C=(1/30)C_{max}$, at $t=t_c$ [-]
D_i : impeller diameter [cm]
D_T : inside diameter of column [cm]
E_c : axial dispersion coefficient for continuous phase [cm^2/min]
F : volumetric flow rate [cm^3/min]
H : plate spacing [cm]
I : injection rate of tracer [g-mole/cm^3 sec]
K : exponential factor [-]
L : column length [cm]
m : fraction of total free area [-]
N : agitator speed (RPM) [min^{-1}]
NO : mesh number [-]
OPT: optimized by regression analysis
P : Peclet number for continuous phase [-]
r : rate of generation by chemical reaction
R : radial position [cm]
R_i : injection tube radius [cm]
S : rate of input by sources [g-mole/cm^{3}min]
ss : sample variance
t : time [min]
t_c : time when concentration is C_T [min]
t_A : time when concentration is C_A [min]
$\bar{t}$: holding time [min]
u : superficial velocity [cm/min]
VAR: variance
x : axial coordinate [cm]
X : matrix of independent variable (X_{ij})
y_i : response
Y : response vector
z : dimensionless axial length [-]

Greek Letters

α : area under response curve
β : regression coefficient
$/\beta$: regression coefficient vector
ε : error
E : error vector
Φ : fractional hold-up
μ : mean (1st moment)
δ : delta function
σ^2 : variance
∇ : gradient

Subscripts

a : entrance or upstream section
b : exit or downstream section
c : continuous phase
d : dispersed phase
e : end of column test section
exp : experimental
i : species
o : injection point or the first of two measurement points

REFERENCES

1. Gutoff, E. B.: *AIChE J.*, **11**, 712 (1965).
2. Miyauchi, T., Mitsutake, H. and Harase, I.: *AIChE J.*, **12**, 508 (1966).
3. Bibaud, R. E. and Treybal, R. E.: *AIChE J.*, **12**, 472 (1966).
4. Oldshue, J. Y. and Rushton, J. H.: *Chem. Eng. Progr.*, **48**, 297 (1952).
5. Zhang, S. H., Ni, X. D. and Su, Y. F.: *Can. J. Chem. Eng.*, **59**, 573 (1981).
6. Laddha, G. S., Degaleesan, T. E. and Kannappan, R.: *Can. J. Chem. Eng.*, **56**, 137 (1978).
7. Kim, S. D. and Baird, M. H. I.: *Can. J. Chem. Eng.*, **54**, 81 (1976).
8. Prochazka, J., Landau, J., Souhrada, F. and Heyberger, A.: *Brit. Chem. Eng.*, **16**, 405 (1971).
9. Novotny, P., Prochzka, J. and Landau, J.: *Can. J. Chem. Eng.*, 48 (1970).
10. Baird, M. H. I.: *Can. J. Chem. Eng.*, **52**, 750 (1974).
11. Shemel, G. A. and Babb, A. L.: *I & EC Pro. Des. and Dev.*, **3**, 210 (1964).
12. Rosen, A. M. and Krylor, V. S.: *Chem. Eng.*, **7**, 85 (1974).
13. Wiegandt, H. F. and Vanberg, R. L.: *Chem. Eng.*, 61 (July, 1954).
14. Thorton, J. D.: Chem. Eng. Progr. Symp. Ser., No.

13, 50, 39 (1954).
15. Seinfeld, J. H. and Lapidus, L.: "Mathematical Method in Chemical Engineering", vol. 3, Prentice-Hall Inc., 305 (1974).
16. Levenspiel, O. and Bischoff, K. B.: "Advances in Chemical Engineering", vol. 4, Academic Press, 95 (1963).
17. Van deer Laan, E. T.: *Chem. Eng. Sci.*, **7**, 187 (1958).
18. Aris, R.: *Chem. Eng. Sci.*, **9**, 266 (1959).
19. Bischoff, K. B.: *Chem. Eng. Sci.*, **12**, 69 (1960).
20. Jeong, G. H.: M. S. Thesis, Ajou Univ. (1983).
21. Kim, C. S.: M. S. Thesis, KAIST (1981).
22. Bischoff, K. B. and Levenspiel, O.: *Chem. Eng. Sci.*, **17**, 245, 257 (1962).
23. Montgomery, D. C.: "Design and Analysis of Experiments", John Wiley & Sons, New York, 304 (1967).
24. Venkataramana, J., Degaleesan, T. E. and Laddha, G. S.: *Can. J. Chem. Eng.*, **58**, 206 (1980).